ISBN: 978-3-95450-247-9 ISSN: 2673-5490 doi: 10.18429/JACoW-IPAC2024-MOPG68

CHARACTERIZATION OF A SINGLE-PASS HIGH-GAIN THz FEL AT PITZ*

M. Krasilnikov †, N. Aftab, Z. Amirkhanyan, D. Dmytriiev, J. Good, A. Grebinyk, M. Gross, A. Hoffmann, D. Kalantaryan, M. Kelisani, E. Kongmon[1], X.-K. Li, Z. Lotfi, A. Lueangaramwong[2], S. Mohanty, A. Oppelt, C. Richard, F. Riemer, E. Schneidmiller, F. Stephan, G. Vashchenko, D. Villani, M. Yurkov, E. Zapolnova, S. Zeeshan, X. Zhang,
Deutsches Elektronen-Synchrotron DESY, Zeuthen and Hamburg, Germany
[1]on leave from Chiang Mai University, Chiang Mai, Thailand
[2]now at Diamond Light Source Ltd, Didcot, UK

Abstract

A single-pass THz free-electron laser (FEL) at the Photo Injector Test facility at DESY in Zeuthen (PITZ) was designed and realized for proof-of-principle experiments on a tunable high-power THz source for pump-probe experiments at the European XFEL. THz pulses are generated at a radiation wavelength of ~100 µm within a 3.5 m long, strongly focusing planar LCLS-I undulator. High gain is achieved by driving the FEL with high brightness beams from the PITZ photoinjector at ~17 MeV and a bunch charge of up to several nC. The experimental results, including the gain curves and spectral properties of the THz-FEL radiation, are presented in comparison with theoretical predictions and numerical simulations.

INTRODUCTION

The pump-probe technique, one of the most advanced tools for experiments at modern XFELs, utilizes two pulses with controlled time delay. Applying this technique, a sample of nonequilibrium states is excited by e.g. intensive THz radiation and probed by delayed X-ray pulse.

Since the most advanced XFEL facilities, such as the European XFEL and the LCLS-II, are based on superconducting technology, THz pulses with repetition rates from 0.1 MHz to 4.5 MHz are also required. Generation of THz pulses with high pulse energy at such a high duty cycle using conventional femtosecond lasers by optical rectification [1] does not allow to achieve the required parameters combining repetition rate AND high pulse energy. Relativistic electron beams can generate electromagnetic radiation over a wide range of wavelengths, from mm to µm to X-rays. And modern accelerators are capable of producing a fairly dense pulse train structure. Therefore, accelerator-based THz sources are considered as possible solutions for pump-probe experiments. A photoinjector-based THz source for pump-probe experiments at the X-ray FEL becomes a natural solution due to all the advantages of accelerator-based THz sources, such as clean in-vacuum production of THz radiation, continuous wavelength tunability, flexibility of the time pattern and spectral characteristics by manipulating the electron beam, as well as polarization control. The use of a RF photogun, identical to the photoinjector at the XFEL accelerator, provides full compatibility of the THz radiation pulse structure with X-ray radiation. The ability to generate high beam charge with modern RF photoguns offers perspectives for increasing the energy of THz pulses up to the level of mJ per bunch.

Developments of a prototype for a high-power tunable accelerator-based THz source for pump-probe experiments at the European XFEL are ongoing at the Photo Injector Test Facility at DESY in Zeuthen (PITZ) [2]. As PITZ is developing the high brightness electron source for the European XFEL accelerator, it makes it possible to generate THz pulses with a pulse repetition rate and a pulse train structure identical to that of the X-ray pulses. High THz SASE FEL radiation power can be achieved by utilizing high charge (up to several nC) electron bunches from the PITZ RF photogun. The first lasing at a central wavelength of ~100 µm was achieved in August 2022 [3]. Further optimization of THz radiation from the THz FEL at PITZ resulted in a significant improvement of the THz source performance [4]. THz pulse energy optimization is currently being performed at two diagnostic stations. This paper reports the characterization of the THz radiation, including gain curves along the undulator, shot-to-shot statistics, and first spectral measurements.

THz BEAMLINE

The THz beamline has been installed as an extension of the existing PITZ linac in the tunnel annex [5]. The PITZ accelerator (Fig. 1) consists of an RF photogun and an RF booster cavity, both standing wave resonators operating at 1.3 GHz and powered by two separate 10 MW klystrons.

A planar LCLS-I undulator [6] is used to generate the THz radiation. The undulator parameters (period of 30 mm and undulator parameter of ∼3.5) require an electron beam energy of ∼17 MeV for the centre radiation wavelength of ∼100 µm. The undulator strong magnetic field with a horizontal gradient requires a thorough beam matching. Another challenge is the narrow vacuum chamber (5 mm height, 11 mm width, and ∼3.5 m length), which makes matching and transport of the space charge dominated electron beams a complex task. A special procedure was developed and experimentally implemented at the newly installed THz beamline [7]. This method is based on an iterative measurement procedure and forward and backward simulations.

* Work supported by the R&D program of the European XFEL
† mikhail.krasilnikov@desy.de

ISBN: 978-3-95450-247-9 ISSN: 2673-5490 doi: 10.18429/JACoW-IPAC2024-MOPG68

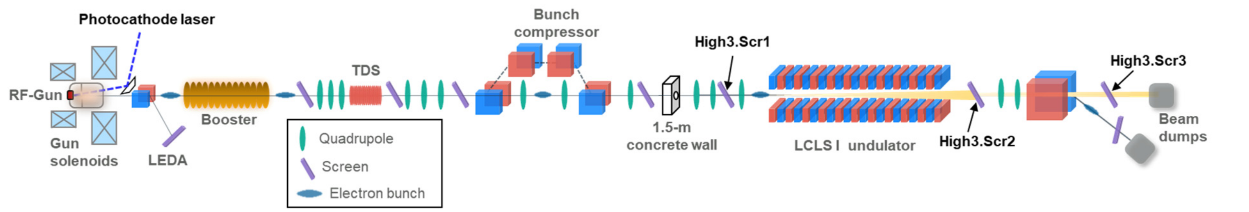

Figure 1: PITZ machine layout (not to scale). The beam travels from the RF gun through the booster, electron beam transport beamline, bunch compressor, the LCLS-I undulator, and THz diagnostic section.

The matching procedure involves quasi-round electron beam transport through a 1.5-meter concrete (Fig. 1) wall with only the beam pipe and no focusing elements, and challenging beam matching conditions at the entrance to the undulator. The design horizontal and vertical Twiss parameters are rather asymmetric and have relatively small acceptance.

The matching of the high charge electron beam into the LCLS-I undulator requires the following transverse beam parameters: the rms beam sizes $\sigma_x \approx 1.3$ mm and $\sigma_y \approx 0.2$ mm, the corresponding beta-functions $\beta_x \approx 10.9$ m and $\beta_y \approx 0.4$ m, which corresponds to a flat beam configuration at the undulator entrance. A bunch charge of 2 nC is considered as a reference case. The experimental electron beam distributions at the YAG screens around the undulator (High3.Scr1 and High3.Scr2 in Fig. 1) are shown in Fig. 2. The beam mean momentum is ~17 MeV/c.

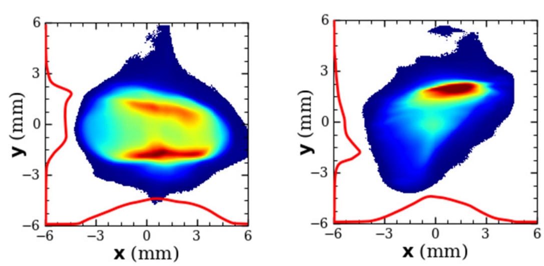

Figure 2: Transverse distributions of a 2 nC electron beam. Left: Upstream of the undulator (screen High3.Scr1). Right: Downstream of the undulator (screen High3.Scr2).

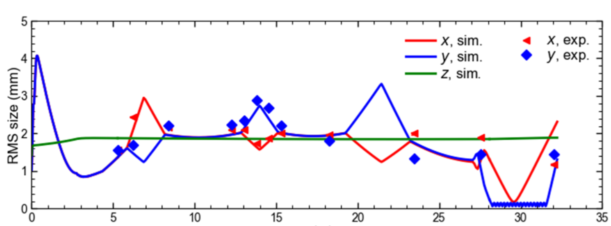

Figure 3: Beam envelope along the PITZ accelerator for 2 nC, 17 MeV/c electron bunch. Solid curves: simulated RMS beam sizes; markers: transverse RMS beam sizes measured at the screen stations along the beamline.

The measured electron beam distributions are in a reasonable agreement with simulation results. A typical 2 nC beam envelope (rms beam sizes) simulated along the beamline with ASTRA code [8] is shown in Fig. 3. The plot also shows experimental data: the rms beam sizes measured at the available screen stations. The slightly increased discrepancy between experiment and modelling along the beamline is mainly due to imperfections such as inhomogeneities in the transverse beam distribution and wakefields that were not included in the simulations

THz DIAGNOSTICS

The THz radiation measurement setup after the undulator consists of two stations named TD2 (associated with High3.Scr2 screen station) and TD3 (associated with High3.Scr3), a dipole magnet, and a beam dump (Fig. 1). A more detailed schematic of THz diagnostics is shown in Fig. 4.

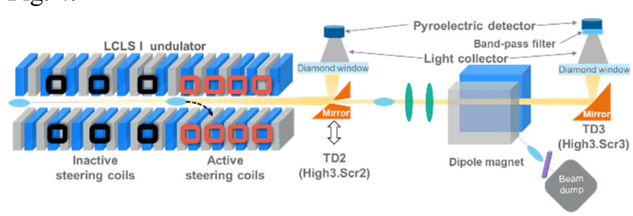

Figure 4: Schematic of the THz diagnostic stations and gain curve measurement setup. Seven steering coils are distributed along the undulator to enable gain curve measurements.

Each screen station has an in-vacuum gold-coated ellipsoidal mirror for transporting the photon beam from the beamline through a diamond window to a pyrodetector. The mirrors can be moved remotely in and out from the beamline using linear motorized stages. The diamond window has a clear aperture of 20 mm and has a flat transmission of >70% for a wavelength longer than 10 µm. The mirror at TD2 has a diameter of 50.8 mm with a 5 mm to 8 mm conical hole that allows the electron beam to pass through. The electron beam is then bent to the beam dump using the dipole magnet. Therefore, only the photon beam can travel to the mirror at TD3. This mirror also has a diameter of 50.8 mm but without a hole. Each screen station has a THz photon diagnostic setup installed at the diamond window's exit. A band-pass filter (BPF3.0-24 Tydex) with maximum transmission of ~92%, centered at 102 µm and a bandwidth of ~12 µm (FWHM) was mounted on top of a cylindrical adapter in front of the pyrodetector at TD3. The THz radiation collection efficiency was estimated by light propagation in a free space to be 49% and 63% for TD2 and TD3, respectively [9].

There is a set of specially designed steering coils distributed along the undulator (Fig. 4). They allow to kick an electron bunch horizontally away from the nominal trajectory in the undulator to measure the THz pulse energy

ISBN: 978-3-95450-247-9 ISSN: 2673-5490 doi: 10.18429/JACoW-IPAC2024-MOPG68

radiated until the kick location (active undulator length), which provides a gain curve. The last four coils are more concentrated in the second part of the undulator to provide more points of a gain curve near where saturation is expected to occur.

THz FEL RADIATION MEASUREMENTS

As mentioned in the previous section, the gain curve measurement procedure is based on the use of short steering coils. Starting with the last coil, all coils one after another are set to a current of +3 A (active steering coils in Fig. 4) which is supposed to kick the beam from the lasing trajectory (in fact, the beam is dumped on the wall of the vacuum chamber). The response time of pyroelectric detectors lies in the range of tens of ms, so it was preferable to use a single bunch in a bunch train with a repetition rate of 10 Hz to measure the THz pulse energy statistics.

Gain Curve Measured at TD2

THz radiation pulse energy of up to ~30 μJ were measured a TD3 (High3.Scr3) with a 3 THz band-pass filter after optimization of the 1-3 nC electron beam trajectory and matching into the undulator [4]. Similar studies were performed at TD2 (High3.Scr2), which is located just after the undulator exit and the station is not equipped with a band-pass filter. Such a setup without band-pass filter implies, on the one hand, the possibility of detecting higher order odd harmonics (third and fifth) over the main wavelength of µm. A very rough estimate based on a linear model gives a contribution of higher-order harmonics of less than 10% to the total generated radiation. On the other hand, the radiation loss through the hole in the mirror is much higher for higher harmonics, and their detection ratio at TD2 is significantly lower. Despite the fact that the in-vacuum mirror of this station has a 5 mm diameter hole for the electron beam to pass through, a significant radiation pulse energy was detected. The gain curve for ∼100 µm center wavelength obtained using 2 nC electron bunches is shown in Fig. 5. The estimated FEL gain of 10^5-10^6 indicates a high-gain THz FEL, which agrees well with theoretical expectations and numerical simulations [4]. The onset of saturation of the gain curve can also be stated.

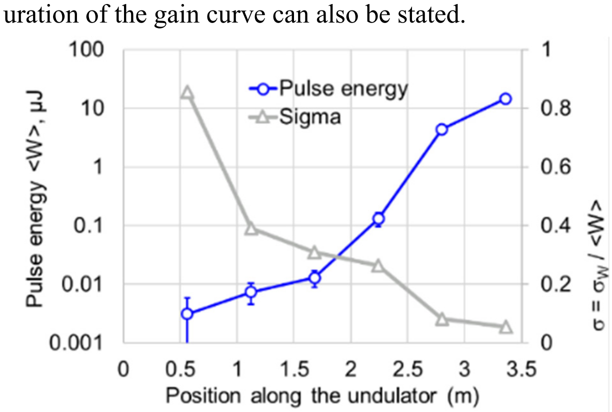

Figure 5: Gain curves measured for 2 nC at TD2 (in-vacuum mirror with a hole) without band-pass filter: mean THz pulse energy $\langle W \rangle$ (left axis) and relative pulse energy fluctuation rate $\sigma_W / \langle W \rangle$ (right axis).

THz Pulse Energy: TD2 Versus TD3

The THz pulse energies measured at different diagnostic stations using 500-shots statistics is shown in Fig. 6. The last point of the gain curve (Fig. 5) was used. It has been observed, that a significant fraction of the radiation passed through the 5 mm-hole in the vacuum mirror at TD2 (High3.Scr2) and was captured by a pyro-detector at TD3 equipped with a whole vacuum mirror. Fig. 6 shows histograms of the measured pulse energy recorded at various THz stations. The pyro detector at TD2 measured an average pulse energy of 15 µJ, while 5 µJ was detected at TD3. A total pulse energy of 22 µJ was detected at TD3 when the in-vacuum mirror at TD2 (High3.Scr2) was removed. This radiation pulse energy is lower than the maximum value of ~30 µJ measured at this station with a band-pass filter [4], which can be explained by imperfect beam matching into the undulator and the slightly lower bunch charge used to obtain the results shown in Fig. 6.

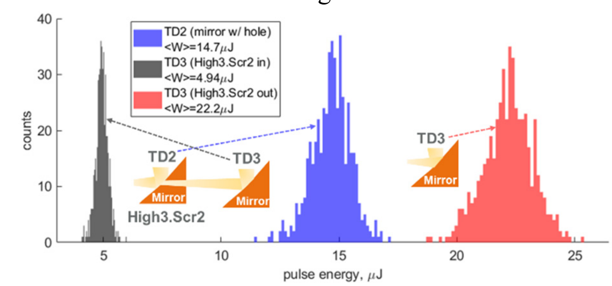

Figure 6: Histograms of 500-shot statistics measured for 2 nC beam at different THz diagnostics stations for various mirror setups at TD2 (in-vacuum mirror with a hole at High3.Scr2).

First Spectral Measurements

The first spectral measurements were performed at the TD3 station using an FTIR (Fourier Transform Infrared) spectrometer based on a reflective lamellar grating [10]. A narrow-band spectrum centered at 2.82 THz was measured, and a FWHM bandwidth of ~1.7% was estimated. In addition, higher odd harmonics were detected. These observations are in good agreement with theoretical expectations and together with measured high gain.

CONCLUSION

A single-pass high-gain THz FEL with electron bunch lengths significantly longer than the radiation wavelength was demonstrated at the photoinjector test facility at DESY in Zeuthen (PITZ). A special procedure for the strongly space charge dominated beam transport and matching into the LCLS-I undulator has been developed and successfully applied. The reference case of a 2 nC electron beam with a mean beam momentum of ~17 MeV/c for FEL radiation at the fundamental frequency of ~3 THz was characterized by the FEL gain curve, cross measurements of THz radiation at various diagnostic stations, and complemented by the first spectrum measurements. High gain and narrow bandwidth were demonstrated using electron beams from the high brightness photo injector, making such a THz source attractive for pump-probe experiments at modern XFELs.

ISBN: 978-3-95450-247-9 ISSN: 2673-5490 doi: 10.18429/JACoW-IPAC2024-MOPG68

REFERENCES

[1] J. Hebling, G. Alm´asi, I. Z. Kozma, and J. Kuhl, "Velocity matching by pulse front tilting for large-area THz-pulse generation," *Opt. Express,* vol. 10, no. 21, p. 1161–1166, 2002.

[2] E. A. Schneidmiller, M. V. Yurkov, M. Krasilnikov, and F. Stephan, "Tunable IR/THz source for pump probe experiments at the European XFEL," *Advances in X-ray Free-Electron Lasers II: Instrumentation,* vol. 8778, pp. 151-156, 2013.

[3] M. Krasilnikov *et al*., "First lasing of the THz SASE FEL at PITZ," in *Proc. 40th Int. Free Electron Laser Conference (FEL2022)*, Trieste, Aug. 2022, pp. 4-6. doi:10.18429/JACoW-FEL2022-MOA08

[4] M. Krasilnikov *et al*., "THz SASE FEL at PITZ: lasing at a wavelength of 100 µm", *J. Phys. Conf. Ser.,* vol. 2687, p. 032016, Jan. 2024. doi:10.1088/1742-6596/2687/3/032016

[5] T. Weilbach *et al*., "Status of the THz@PITZ Project - The Proof-of-Principle Experiment on a THz SASE FEL at the PITZ Facility," in *Proc. IPAC'22*, Bangkok, Jun. 2022, pp. 1033-1036. doi:10.18429/JACoW-IPAC2022-TUPOPT016

[6] E. Trakhtenberg *et al*., "Undulator for the LCLS project—from the prototype to the full-scale manufacturing," *Nucl. Instrum. Methods Phys. Res., Sect. A,* vol. 543, no. 1, pp. 42-46, 2005. doi:10.1016/j.nima.2005.01.110

[7] X.-K. Li *et al*., "Matching of a space-charge dominated beam into the undulator of the THz SASE FEL at PITZ," in *Proc. 12th Int. Particle Acc. Conf. (IPAC'21)*, Campinas, SP, Brazil, May 2021, pp. 3234-3247. doi:10.18429/JACoW-IPAC2021-WEPAB257

[8] K. Flöttmann, "ASTRA Particle Tracking Code," [Online], https://www.desy.de/~mpyflo/

[9] P. Boonpornprasert *et al*., "Photon diagnostics for the high-gain THz FEL at PITZ," *J. Phys. Conf. Ser.,* vol. 2687, no. 3, p. 032046, Jan. 2024. doi:10.1088/1742-6596/2687/3/032046

[10] R. Pan *et al*., "Photon diagnostics at the FLASH THz beamline," *J. Synchrotron Radiat.,* vol. 26, no. 3, pp. 700-707, Apr. 2019. doi:10.1107/S1600577519003412